

# Preparation and Properties of NH<sub>2</sub>-SBA-16@IAA@CS Coating

Yidan Yang, Lingyun Luo, Qiang Zhou, Huiyaun Deng, Xiaonan Liu \*

School of Chemical Engineering, Sichuan University of Science & Engineering, Zigong, China

\*Corresponding Author: Xiaonan Liu

## ABSTRACT

In the present study, aminoated SBA-16@indoleacetic acid-@chitosan composite (NH<sub>2</sub>-SBA-16@IAA@CS) was prepared on glass plate (supporting substrate). Indoleacetic acid (IAA) was introduced into aminoized SBA-16 (NH<sub>2</sub>-SBA-16), mixed with chitosan and coated on glass plate to form antibacterial slow-release coating. BET, XRD and FTIR results showed that IAA was successfully introduced into the aminating SBA-16 material. The antibacterial activity of the composite coating was studied using the biofilm-forming bacteria *Bacillus subtilis* and *Escherichia coli*. Under the same conditions, NH<sub>2</sub>-SBA-16@IAA@CS composite coated fiberglass board showed antibacterial activity compared with chitosan. The release time and amount of IAA in the composite material were also tested, and it was found that the release rate of IAA in the prepared composite coating was effectively reduced in the alkaline seawater. NH<sub>2</sub>-SBA-16@IAA@CS composites are promising alternatives to toxic antifouling coatings in the ocean.

## KEYWORDS

SBA-16 composite material; Coating; Sustained release properties; Marine antibacterial

## 1. INTRODUCTION

The Marine industry is booming, and equipment in the ocean can be attached by bacteria and microorganisms, which affects its economic efficiency. In the early stage of attachment of Marine organisms, proteins, polysaccharides and other substances will quickly form a layer of mucous membrane on the surface of the equipment [1-2], and Marine microorganisms (such as bacteria, diatoms, protozoa, etc.) will begin to multiply and grow on the formed mucous membrane [3], and then serious biological fouling will occur. These biological fouling will produce high friction resistance, increase the fuel consumption of the ship, and also reduce the speed of the ship [4-5]. The cost of cleaning a ship in the military industry can be as high as \$56 million per year, while in the aquaculture industry cleaning costs account for 5-10% of production costs [6-7]. Addressing the growth of biological fouling can avoid some economic losses.

Bioluminescence can be controlled by coating the material with substances or materials that inhibit its growth [8]. Green antibacterial slow release coating is an effective means to prevent the growth of biological fouling. Generally, when bacteria and other microorganisms grow on the material mucosa (that is, in the early stage of a large number of Marine organisms attached), the antibacterial agent released by the coating is used to kill bacteria and other microorganisms, destroy the environment for subsequent Marine organisms to attach, and can effectively prevent the growth of biological dirt, and there are no disadvantages such as uneven release speed and short antifouling time when conventional materials release antimicrobials. In addition, most commercial antifouling paints contain highly toxic fungicides, which may affect the reproduction process and behavior of fish even at low concentrations [9-10], while the antibacterial agents used in green antibacterial slow-release coatings have low

mechanical and thermal toxicity and are easy to process, which will not have a bad impact on the normal life activities of organisms. As one of the natural products, IAA has the characteristics of good biocompatibility and low toxicity.

Some plant polysaccharides have been shown to have strong antibacterial activity against various gram-negative and Gram-positive bacteria [11]. As a plant polysaccharide, CS not only has good antibacterial activity, but also is easy to form film. CS is a biopolymer derived from chitin and is known for its strong antifungal activity while being biodegradable, biocompatible and non-toxic [12]. By modifying the surface of mesoporous silica SBA-16 with amino group, the tight binding with IAA can be enhanced, so as to improve the loading capacity and slow release performance of IAA. SBA-16 is a pure silica mesoporous molecular sieve with uniform pore distribution that can control the release rate of indoleacetic acid and no metal ions flow into the ocean. The addition of IAA molecular sieve into CS can enhance the antibacterial activity of pure CS coating and delay the release rate of IAA, so it can be applied in many fields, such as coating on Marine culture glass or other equipment. Even if used in large quantities in the Marine environment, it will not cause Marine pollution similar to that caused by heavy metal fungicides.

Therefore, in this paper, we prepared chitosan coating with slow release indoleacetic acid to overcome the disadvantages of high toxicity and short aging of conventional antifouling coatings. It provides an idea for the exploration of green antibacterial coating.

## **2. PREPARATION OF HYDROGEL AND PTFE COMPOSITE MATERIALS**

### **2.1. Materials**

Chitosan (CS), 3-Indoleacetic acid (IAA), gelatin, N-[3-(Trimethoxysilyl) propyl] ethylenediamine, SBA-16, methylbenzene, Acetone. All reagents utilized in this study are of analytical grade purity, ensuring their suitability for high-quality research applications.

### **2.2. Preparation of NH<sub>2</sub>-SBA-16**

1g SBA-16 and 0.6g N-[3-(Trimethoxysilyl) propyl] ethylenediamine were heated in 70mL toluene solvent at 70-90°C for 12 hours, then pumped and filtered into a vacuum drying oven at 70°C for 5 hours to obtain NH<sub>2</sub>-SBA-16 white powder.

### **2.3. Preparation of NH<sub>2</sub>-SBA-16@IAA**

The mass ratio of 1g NH<sub>2</sub>-SBA-16 to IAA was 2:1, 1:1 and 1:2, respectively, when IAA was added to 1G NH<sub>2</sub>-SBA-16 with 30mL acetone as solvent and heated and stirred at 30°C for 10h. After spinning steaming, the solution is washed with the corresponding solvent, put into a vacuum drying oven at 30°C for 5h, and then take out to obtain reddish-brown NH<sub>2</sub>-SBA-16@IAA; Similarly, after replacing NH<sub>2</sub>-SBA-16 with SBA-16, other conditions remain unchanged, the reddish-brown SBA-16@IAA is obtained.

### **2.4. Preparation of NH<sub>2</sub>-SBA-16@IAA@CS**

1gNH<sub>2</sub>-SBA-16@IAA was put into 20mL gelatin solution with a concentration of 50mg/mL, and then into a constant temperature shaking table at 30°C for 5h, centrifugally washed with deionized water at 4°C for two times, and then dried at 30°C for 12h to obtain NH<sub>2</sub>-SBA-16@IAA @gelatin. Add 1gCS into 100mL (1%V) acetic acid solution and disperse evenly into 10mg/mL CS solution; add 0.5g NH<sub>2</sub>-SBA-16@IAA @gelatin into 20mLCS solution with a concentration of 10mg/mL, stir for 1h, and then pour into the petri dish. Put into a vacuum drying oven at 35°C for 12h to get NH<sub>2</sub>-SBA-16@IAA@CS coating.

### 3. PERFORMANCE EVALUATION

#### 3.1. Release of IAA

50mg NH<sub>2</sub>-SBA-16@IAA, 50mg NH<sub>2</sub>-SBA-16@IAA@CS, and SBA-16@IAA50mg were added into 100mL artificial seawater, respectively. The concentration change of indoleacetic acid in seawater was continuously measured by ultraviolet spectrophotometer with the detection wavelength of 221nm.

#### 3.2. Anti-Pollution Performance Testing

After preparing the fresh culture of *Bacillus subtilis*, the bacterial culture was grown at 37°C for 24 hours. The 24 panels (1cm×1cm) were divided into 7 groups with 3 panels in each group. One group of panels was coated with CS, and the three groups were coated with mass ratios of 2:1, 1:1, and 1 respectively: The remaining three groups were respectively coated with NH<sub>3</sub>-SBA-16@IAA@CS composite coating prepared by mixing CS with the first three kinds of NH<sub>3</sub>-SBA-16@IAA. Using CS coating as a negative control, 3mL sterile Marine broth was mixed with a bacterial culture of *Bacillus subtilis* with a concentration of about 10 CFU (colony forming unit) /mL, and added into each well to measure the amount of CFU in all treatments after 0 hours and 24 hours, as shown in Figure 4.

Similarly, the above operations were carried out by changing the bacterial culture from *Bacillus subtilis* to *E. coli*, and the results were shown in Figure 5.

### 4. RESULTS AND DISCUSSION

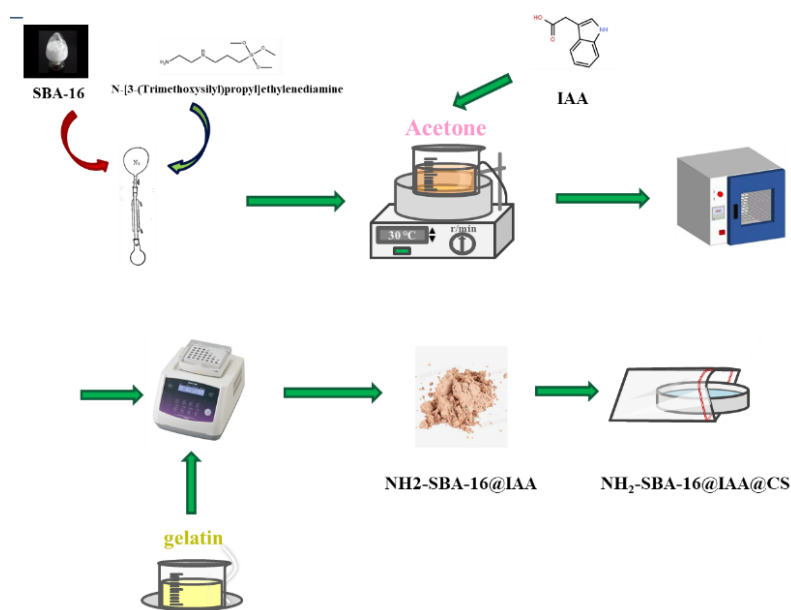


**Figure 1.** NH<sub>2</sub>-SBA-16@IAA@CS of coating preparation process

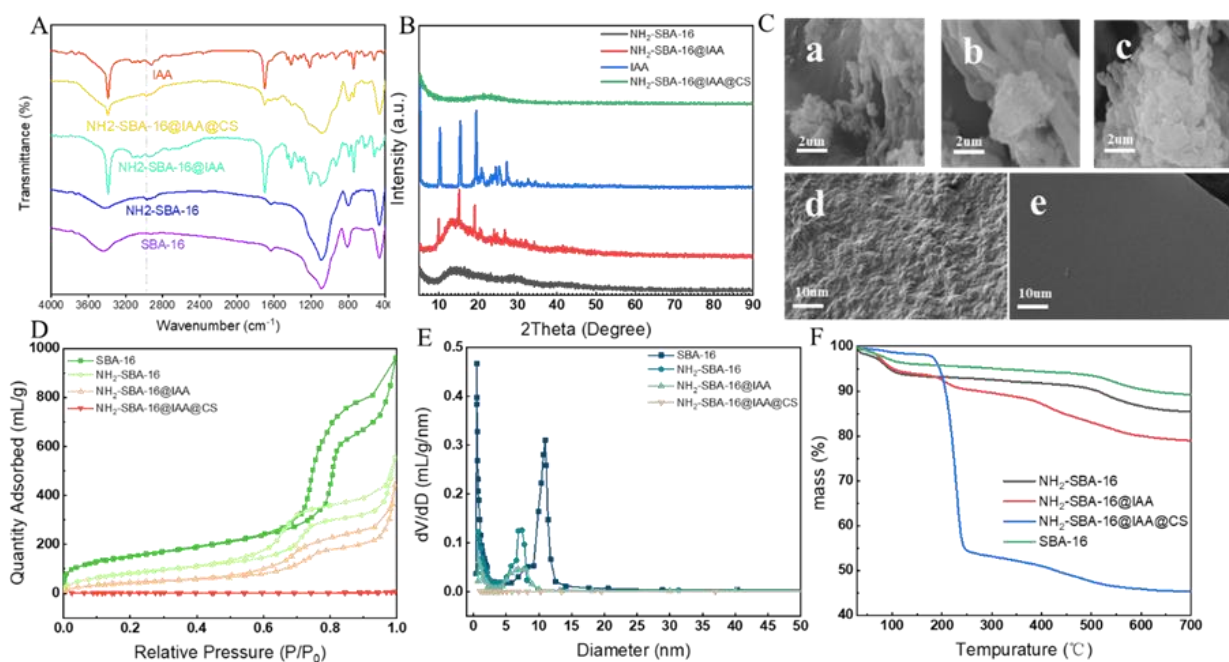


**Figure 2.** A) FT-IR diagram of materials SBA-16, NH<sub>2</sub>-SBA-16, NH<sub>2</sub>-SBA-16@IAA, IAA and NH<sub>2</sub>-SBA-16@IAA@CS; B) XRD patterns of NH<sub>2</sub>-SBA-16, NH<sub>2</sub>-SBA-16@IAA, IAA and NH<sub>2</sub>-SBA-16@IAA@CS materials; C) SEM diagram of SBA-16 b.NH<sub>2</sub>-SBA-16 c.NH<sub>2</sub>-SBA-16@IAA D.D.C e.NH<sub>2</sub>-SBA-16@IAA@CS; D) BET N<sub>2</sub> adsorption-desorption of SBA-16, NH<sub>2</sub>-SBA-16, NH<sub>2</sub>-SBA-16@IAA and NH<sub>2</sub>-SBA-16@IAA@CS; E) Pore size distribution of SBA-16, NH<sub>2</sub>-SBA-16, NH<sub>2</sub>-SBA-16@IAA and NH<sub>2</sub>-SBA-16@IAA@CS materials; F) Thermogravigram of SBA-16, NH<sub>2</sub>-SBA-16, NH<sub>2</sub>-SBA-16@IAA and NH<sub>2</sub>-SBA-16@IAA@CS materials

The infrared spectra of SBA-16, NH<sub>2</sub>-SBA-16, NH<sub>2</sub>-SBA-16@IAA, NH<sub>2</sub>-SBA-16@IAA@CS and IAA are shown in Figure 2A. It can be seen from the figure that IAA has a strong absorption peak at 1698cm<sup>-1</sup>, which belongs to the carbonyl stretching vibration absorption peak in IAA. Among them, a series of absorption peaks in the range of 1400~1600cm<sup>-1</sup> are the peaks caused by the skeleton vibration of the benzene ring in IAA, which verifies that IAA belongs to the carboxylic acids with benzene ring. According to the spectrogram analysis of SBA-16, it can be seen that the absorption peaks mainly appear around 3400 cm<sup>-1</sup>, 1100 cm<sup>-1</sup> and 800 cm<sup>-1</sup>, and the absorption peaks around 3400 cm<sup>-1</sup> belong to the characteristic peaks of alcohols in Si-O-H bond. The peaks around 1100 cm<sup>-1</sup> and 800 cm<sup>-1</sup> are characteristic peaks of Si-O-Si bond. The weak absorption peak of 2975 cm<sup>-1</sup> was found in the figure of NH<sub>2</sub>-SBA-16, which is the C-H vibration peak of the saturated alkane in the coupling agent.

The XRD patterns of NH<sub>2</sub>-SBA-16, NH<sub>2</sub>-SBA-16@IAA, NH<sub>2</sub>-SBA-16@IAA@CS and IAA are shown in Figure 2B. The dispersibility of IAA in composite materials can be studied by observing the spectrum. NH<sub>2</sub>-SBA-16 material appears a wide diffraction peak at about 10~30° is the characteristic diffraction peak of amorphous silica, and other diffraction peaks do not appear. Diffraction peaks of 10.2°, 15.4°, 19.5° and 27.3° appear on the spectra of IAA. For NH<sub>2</sub>-SBA-16@IAA, there are not only the characteristic diffraction peaks of amorphous silica NH<sub>2</sub>-SBA-16, but also a series of diffraction peaks of IAA. It is shown that IAA is successfully loaded onto NH<sub>2</sub>-SBA-16 without affecting the structure of mesoporous silica. However, the diffraction peaks of IAA and NH<sub>2</sub>-SBA-16 on the NH<sub>2</sub>-SBA-16@IAA@CS spectrum disappear, which proves that CS is uniformly wrapped on NH<sub>2</sub>-SBA-16@IAA material, and NH<sub>2</sub>-SBA-16@IAA material itself is not missed outside CS, and is completely wrapped. It is matched with the greatly reduced IAA release rate.

It can be seen that SBA-16 in Figure 2Ca, NH<sub>2</sub>-SBA-16 in Figure 2Cb, and NH<sub>2</sub>-SBA-16@IAA in Figure 2Cc did not damage the structure and function of the molecular sieve itself. Despite surface

functionalization, ordered mesoporous structures with uniform cubic symmetric ( $Im\bar{3}m$ ) pore structures have been observed over a wide range [141-142]. The introduced amino groups were slightly agglomerated on the surface of SBA-16, forming fine particles and slightly agglomerating. The subsequent addition of IAA increased the agglomerating degree. In Figure 2C, d and e are pure chitosan coating and composite coating with NH<sub>2</sub>-SBA-16@IAA added, respectively. It can be obviously observed that the coating formed by CS is in good film form and has a very smooth surface. However, the surface of the coating is uneven after NH<sub>2</sub>-SBA-16@IAA is added.

As can be seen from the N<sub>2</sub> adsorption isotherm curves of SBA-16, NH<sub>2</sub>-SBA-16, NH<sub>2</sub>-SBA-16@IAA and NH<sub>2</sub>-SBA-16@IAA@CS shown in Figure 2D, The three materials, SBA-16, NH<sub>2</sub>-SBA-16 and NH<sub>2</sub>-SBA-16@IAA, conform to the type IV in the adsorption isotherm, and the accompanying H<sub>2</sub> type hysteresis can be observed. This characteristic belongs to mesoporous materials prepared by non-ionic surfactants, and is also the embodiment of cage pores, which proves that neither amino modification nor IAA loading has any effect on the cage structure of SBA-16. In the adsorption-desorption curve, SBA-16 has the largest retention ring and pore volume of all materials in the range of  $0.6 \leq P/P_0 \leq 1$ . After modification, the ring and pore volumes of NH<sub>2</sub>-SBA-16 materials are reduced compared with the original ones. On the other hand, NH<sub>2</sub>-SBA-16@IAA still retains ring and pore volume after IAA loading, but compared with SBA-16 and NH<sub>2</sub>-SBA-16, both ring and pore volume are smaller. As can be seen from the figure, both the specific surface area and pore volume of NH<sub>2</sub>-SBA-16@IAA@CS are very small, almost 0. Because CS completely covers the material NH<sub>2</sub>-SBA-16@IAA, the original NH<sub>2</sub>-SBA-16@IAA channels are completely blocked, which makes the material lose the characteristics of cage channels of mesoporous materials. The results showed that the combination of CS and gelatin successfully blocked the aminating SBA-16 mesoporous material loaded with IAA, thereby slowing down the release rate of IAA.

The same result as the adsorption isothermal curve can be obtained from Figure 2E. It can be seen that the pore size distribution range of materials is narrow and concentrated in mesoporous pore size, and the approximate pore size range is 5-15nm, which indicates that the pore size distribution of SBA-16, NH<sub>2</sub>-SBA-16 and NH<sub>2</sub>-SBA-16@IAA is uniform. And the aperture is concentrated at about 10nm. Similarly, the pore sizes of these three materials become smaller and smaller with amination and IAA loading, while the pore sizes of NH<sub>2</sub>-SBA-16@IAA@CS directly shrink to 0, which means that NH<sub>2</sub>-SBA-16@IAA is completely blocked by CS, which is also consistent with the results of N<sub>2</sub> adsorption isotherm curve. Through the analysis of the specific surface area, pore size and pore volume of SBA-16, NH<sub>2</sub>-SBA-16, NH<sub>2</sub>-SBA-16@IAA and NH<sub>2</sub>-SBA-16@IAA@CS, it can be seen that the data of the first three materials only decrease to some extent, but that of NH<sub>2</sub>-SBA-16@IAA@CS decreases sharply to almost 0. It was also verified that CS and gelatin cross-linked the NH<sub>2</sub>-SBA-16@IAA with mesoporous pores and uniform distribution of pores, and the porous material was successfully blocked.

Comprehensive analysis verified that NH<sub>2</sub>-SBA-16@IAA@CS was successfully prepared, SBA-16 successfully adsorbed IAA in its mesoporous interior, and the structure of SBA-16 was preserved without being destroyed, and gelatin crosslinking was blocked and successfully dispersed in chitosan.

IAA is the main antibacterial agent, and the study of IAA release efficiency is of great reference significance for the study of antibacterial action and time of its antibacterial coating. The main influencing factors in the ocean are temperature and pH, and these two factors are mainly explored in the experiment. As can be seen from Figure 3a, the prepared NH<sub>2</sub>-SBA-16@IAA@CS coating is mainly investigated at 20°C~60°C, which includes most of the ocean surface temperature. In FIG. a, the release rate of IAA of the coating at 20°C is the lowest, and the release rate at 60°C is the highest. The release rate of IAA of NH<sub>2</sub>-SBA-16@IAA@CS coating also gradually increases with the increase of environmental release temperature, but the overall change trend is relatively stable. This is because in the early stage, the solubility of CS will be increased when the temperature rises, and the release of IAA from the composite coating will be accelerated on the side. Therefore, the release rate is fast before 2d and affected by the solubility of CS, there will be a period of short-term

acceleration of the release rate. After reaching the dissolution equilibrium, the overall release rate will be maintained again at a relatively constant rate.

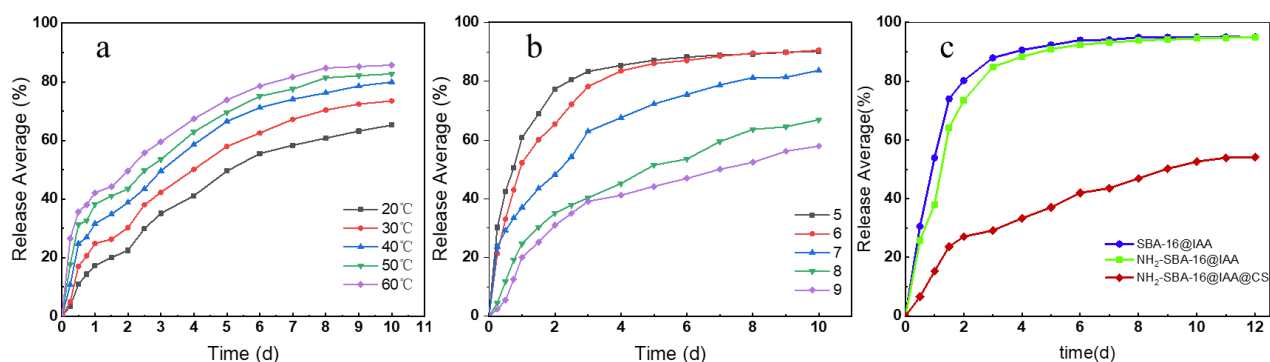


**Figure 3.** a) IAA release amount of NH<sub>2</sub>-SBA-16@IAA@CS coating at different temperatures; b) IAA release amount of NH<sub>2</sub>-SBA-16@IAA@CS coating at different pH; c) Release amount of IAA under different material loads

Figure 3b studies the change of IAA release rate of NH<sub>2</sub>-SBA-16@IAA@CS at a pH of 5-9. It is found that the release rate of IAA decreases obviously and gradually as the pH of the composite coating increases, that is, it changes from acidic to alkaline. When the pH is 5, the release rate exceeds 90% after 6 days. This is because the solubility of chitosan will be greatly increased under acidic conditions, and the higher the acidity is, the better the solubility will be. Therefore, the influence of pH on the composite coating is more obvious. The release rate of IAA under different pH is more significant than that under different temperature environments.

In combination with Figure 3a and 3b, it can be seen that decreasing temperature and increasing pH will slow down the release rate of IAA of the composite coating, thereby increasing the release time and extending the antibacterial time. Therefore, the IAA release rate of different materials at pH 9 and temperature 20°C was investigated in Figure 3c. Compared with unaminated SBA-16, the release rate of aminated SBA-16 decreased. At the same time, the release rate of IAA was greatly reduced after the NH<sub>2</sub>-SBA-16@IAA crosslinked gelatin was mixed with CS, and the purpose of slow release was achieved.

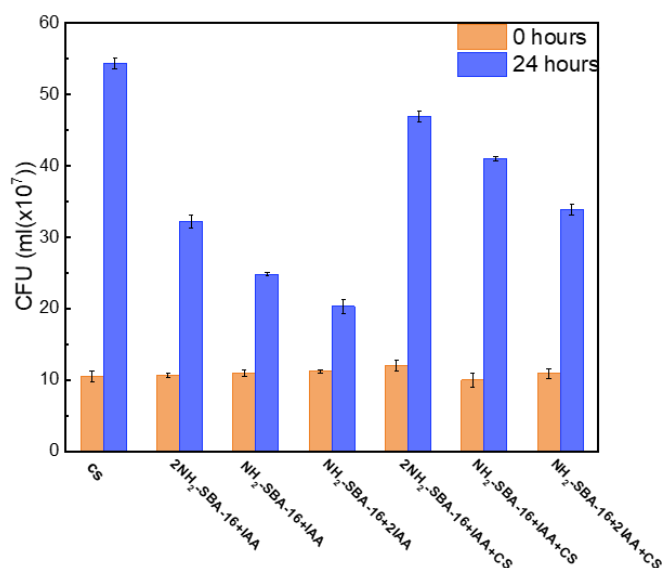


**Figure 4.** Antibacterial activities of CS coating, NH<sub>2</sub>-SBA-16@IAA composite material and NH<sub>2</sub>-SBA-16@IAA@CS composite coating against *Bacillus subtilis*; According to the bacterial growth time of 0h and 24h, the bacterial growth amount was counted by CFU/ml. CS - chitosan coating; xNH<sub>2</sub>-SBA-16+yIAA:NH<sub>2</sub>-SBA-16@IAA composite material, x:y represents the mass ratio; NH<sub>2</sub>-SBA-16+IAA+CS -- NH<sub>2</sub>-SBA-16@IAA@CS composite coating

*Bacillus subtilis* is a major Marine biological pollution bacteria previously isolated from the reverse osmosis membrane of seawater desalination plants, and is also a major component of the Marine bacterial community [13-14]. After 24 hours of bacterial culture, the highest density of *Bacillus subtilis* was observed on the control (pure chitosan coating), while the lowest density was observed on NH<sub>2</sub>-SBA-16@2IAA (NH<sub>2</sub>-SBA-16:IAA mass ratio 1:2) composite. After 24 h culture, the *Bacillus subtilis* density of NH<sub>2</sub>-SBA-16@IAA composite and NH<sub>2</sub>-SBA-16@IAA@CS composite coatings was significantly decreased compared with the control (pure chitosan coating). Of course, NH<sub>2</sub>-SBA-16@IAA has a lower density of *Bacillus subtilis* than NH<sub>2</sub>-SBA-16@IAA@CS composite coating. This is due to the incorporation of NH<sub>2</sub>-SBA-16@IAA composite material into CS, which significantly reduces the release rate of IAA in a short period of time. Combined with the release rate of IAA in NH<sub>2</sub>-SBA-16@IAA and NH<sub>2</sub>-SBA-16@IAA@CS in Figure 3c, it can be seen that The release rate of NH<sub>2</sub>-SBA-16@IAA material is much higher than that of composite coating. Therefore, NH<sub>2</sub>-SBA-16@IAA has better antibacterial performance and the best material is the mass ratio of NH<sub>2</sub>-SBA-16: IAA is 1:2, and the mass ratio is 1: The NH<sub>2</sub>-SBA-16@IAA@CS composite coating prepared by 2's NH<sub>2</sub>-SBA-16@IAA material has stronger antibacterial effect than the composite coating prepared by other proportion NH<sub>2</sub>-SBA-16@IAA material. However, it can also be seen that the antibacterial properties of this series of materials are not good, and some bacillus species are resistant to fungicides [15], which can explain the reasons for the poor performance in our experiment.

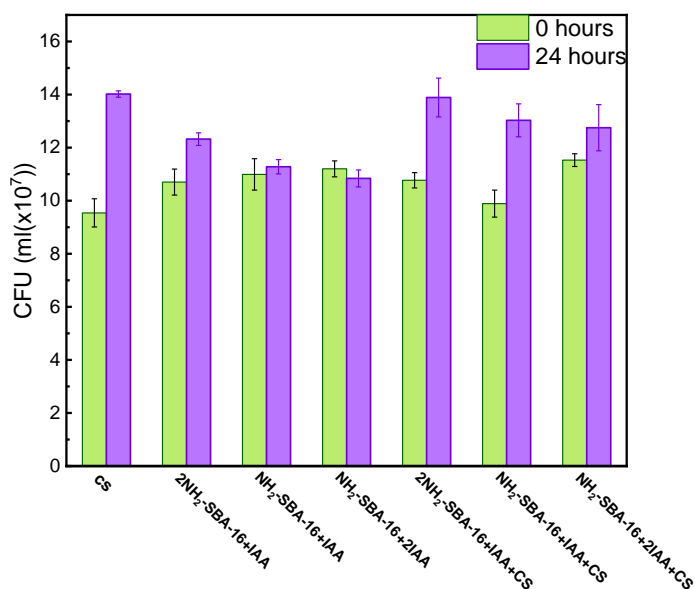


**Figure 5.** Antibacterial activities of CS coating, NH<sub>2</sub>-SBA-16@IAA composite material and NH<sub>2</sub>-SBA-16@IAA@CS composite coating on *E. coli*;

For materials and coatings, the principle of inhibition against *E. coli* is like that of *Bacillus subtilis*. All coatings showed a significant reduction in *E. coli* cells compared to the control (CS). Of course, the lowest bacterial density of the composite coating was consistent with the result obtained by *Bacillus subtilis*, which was still the highest bacterial density in the control (CS). The results showed that the composite coating also had the corresponding antibacterial performance against Gram-negative bacteria (*E. coli*), and the overall antibacterial effect was more significant than that of Gram-positive bacteria (*Bacillus subtilis*). This result can be explained by the difference in cell wall structure between Gram-positive and Gram-negative bacteria [16]. It has long been reported that CS inhibits bacterial growth. Compared with the single outer membrane of Gram-positive bacteria (such as *Bacillus subtilis*), the double outer membrane of *Escherichia coli* has lower permeability to CS [17].

## 5. CONCLUSION

In the present study, the gelatine-coated amino modified porous composite was synthesized by post-encapsulation technique, and the composite coating was obtained by incorporating the material into CS. By various characterization techniques, it was proved that IAA was adsorbed by mesoporous material in NH<sub>2</sub>-SBA-16@IAA composite, and its structure was preserved. CS was uniformly and densely wrapped around NH<sub>2</sub>-SBA-16@IAA to form a composite coating NH<sub>2</sub>-SBA-16@IAA@CS. The IAA release performance of the composite coating was evaluated in the temperature range of 20°C-60°C and pH: 5-9. The results show that the IAA release rate of the composite coating increases with the increase of temperature and decreases with the increase of pH. By comparing the release rates of different materials, it is proved that the release rate of IAA is effectively controlled. Their antifouling activity was tested with gram-positive and Gram-negative bacteria. Compared with pure CS coating, the composite coating showed higher antifouling activity. Composite coatings are more effective at eliminating gram-negative bacteria than Gram-positive bacteria. Combining slow-release materials (NH<sub>2</sub>-SBA-16@IAA) and biodegradable polymers (such as CS) in a single coating is a promising environmentally friendly way to prevent Marine biological pollution. Future field experiments are needed to prove the antifouling effect of NH<sub>2</sub>-SBA-16@IAA@CS composite coating.

## ACKNOWLEDGEMENTS

Thanks to “Sichuan University of Science & Engineering Graduate Student Innovation Fund Project (Y2023043)” for the financial support.

## REFERENCES

- [1] STOWE S D, RICHARDS J J, TUCKER A T, et al. Anti-Biofilm Compounds Derived from Marine Sponges. *Marine Drugs*, 2011, 9(10): p. 2010-2035.
- [2] DAS S. Genetic Regulation, Biosynthesis and Applications of Extracellular Polysaccharides of the Biofilm Matrix of Bacteria. *Carbohydrate Polymers*, 2022, 291.
- [3] SCHULTZ M P, BENDICK J A, HOLM E R, et al. Economic Impact of Biofouling on a Naval Surface Ship. *Biofouling*, 2011, 27(1): p. 87-98.
- [4] Diego Meseguer Yebra, Søren Kiil, Kim Dam-Johansen. Antifouling technology—past, present and future steps towards efficient and environmentally friendly antifouling coatings. *Progress in Organic Coatings*, 2004, 50(2): p. 75-104.
- [5] Aimee L Phillippi, Nancy J O'Connor, Armand F Lewis, et al. Surface flocking as a possible anti-biofoulant. *Aquaculture*, 2001, 195(3-4): p. 225-238.
- [6] Schultz M P, Bendick J A, Holm E R, et al. Economic impact of biofouling on a naval surface ship. *Biofouling*, 27(1): p. 87-98.
- [7] Bannister Jana, Sievers Michael, Bush Flora, et al. Biofouling in marine aquaculture: a review of recent research and developments. *Biofouling*, 2019, 35(6): p. 631-648.
- [8] Dobretsov Sergey, Dahms Hans-Uwe, Qian Peri-Yuan. Inhibition of biofouling by marine microorganisms and their metabolites. 2006, 22(1): p. 43-54.
- [9] Vivien W.W. Bao, Kenneth M.Y. Leung, Jian-Wen Qiu, et al. Acute toxicities of five commonly used antifouling booster biocides to selected subtropical and cosmopolitan marine species. *Marine Pollution Bulletin*, 2011, 62(5): p. 1147-1151.
- [10] Peter Dimitriou, Joanna Castritsi-Catharios, Helen Miliou. Acute toxicity effects of tributyltin chloride and triphenyltin chloride on gilthead seabream, *Sparus aurata* L., embryos. *Ecotoxicology and Environmental Safety*, 2003, 54(1): p. 30-35.
- [11] Zhou Yin, Chen Xinxin, Chen Tingting, et al. A review of the antibacterial activity and mechanisms of plant polysaccharides. *Trends in Food Science & Technology*. 2022, 127: p. 264-280.
- [12] POZNANSKI Pawel, HAMEED Amir, ORCZYK Waclaw. Chitosan and chitosan nanoparticles: parameters enhancing antifungal activity. *Molecules (Basel, Switzerland)*, 2023, 28(7): p. 2996.

- [13] Sergey Dobretsov, Racid M.M. Abed, Max Teplitski, et al. Mini-review: inhibition of biofouling by marine microorganisms. *Biofouling*, 2013, 29(4): p. 423-441.
- [14] Muhammad Abdul Mojid Mondol, Hee Jae Shin, Mohammad Tofazzal Islam. Diversity of Secondary Metabolites from Marine Bacillus Species: Chemistry and Biological Activity. *Mar. Drugs*, 2013, 11(8): p. 2846-2872.
- [15] A.D. Russell. Bacterial resistance to disinfectants: present knowledge and future problems. *Journal of Hospital Infection*, 1999, 43: p. S57-S68.
- [16] Gang Xiao, Xi Zhang, Wanying Zhang, et al. Visible-light-mediated synergistic photocatalytic antimicrobial effects and mechanism of Ag-nanoparticles@chitosan-TiO<sub>2</sub> organic–inorganic composites for water disinfection. *Applied Catalysis B: Environmental*, 2015, 170-171: p. 255-262.
- [17] Ilana Perelshtein, Elena Ruderman, Nina Perkas, et al. Chitosan and chitosan–ZnO-based complex nanoparticles: formation, characterization, and antibacterial activity. *Journal Of Materials Chemistry B*, 2013, 1(14): p. 1968-1976.